

AD-A259 323



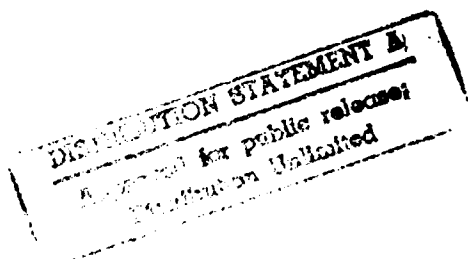
2

ATTENUATION AND SOURCE STUDIES  
IN NORTHERN EURASIA

by

B.J. Mitchell  
J.K. Xie

Department of Earth and Atmospheric Sciences  
Saint Louis University  
221 North Grand Boulevard  
St. Louis, MO 63103



30 December 1992



Semi-Annual Technical Report  
9 January 1992 - 8 July 1992

93-00969



## REPORT DOCUMENTATION PAGE

1a. REPORT SECURITY CLASSIFICATION Unclassified		1b. RESTRICTIVE MARKINGS	
2a. SECURITY CLASSIFICATION AUTHORITY		3. DISTRIBUTION/AVAILABILITY OF REPORT Approved for public release; distribution unlimited.	
2b. DECLASSIFICATION/DOWNGRADING SCHEDULE			
4. PERFORMING ORGANIZATION REPORT NUMBER(S)		5. MONITORING ORGANIZATION REPORT NUMBER(S)	
6a. NAME OF PERFORMING ORGANIZATION Saint Louis University	6b. OFFICE SYMBOL (If applicable)	7a. NAME OF MONITORING ORGANIZATION Defense Advanced Research Projects Agency	
6c. ADDRESS (City, State and ZIP Code) 221 N. Grand Boulevard St. Louis, MO 63103		7b. ADDRESS (City, State and ZIP Code) 3701 N. Fairfax Drive Arlington, VA 22203-1714	
8a. NAME OF FUNDING/SPONSORING ORGANIZATION Defense Advanced Research Projects Agency	8b. OFFICE SYMBOL (If applicable) NMRO	9. PROCUREMENT INSTRUMENT IDENTIFICATION NUMBER FY3592-91-10651	
8c. ADDRESS (City, State and ZIP Code) 3701 N. Fairfax Drive Arlington, VA 22203-1714		10. SOURCE OF FUNDING NOS.	
		PROGRAM ELEMENT NO.	PROJECT NO.
		TASK NO.	WORK UNIT NO.
11. TITLE (Include Security Classification) Attenuation & Source Studies in Northern Eurasia (unclassified)			
12. PERSONAL AUTHOR(S) Brian J. Mitchell			
13a. TYPE OF REPORT Semi-Ann. Technical	13b. TIME COVERED FROM 1/9/92 TO 7/8/92	14. DATE OF REPORT (Yr., Mo., Day) December 30, 1992	15. PAGE COUNT
16. SUPPLEMENTARY NOTATION			
17. COSATI CODES		18. SUBJECT TERMS (Continue on reverse if necessary and identify by block number)	
FIELD	GROUP	SUB. GR.	
		Seismology, Attenuation, Lg, Surface waves	
19. ABSTRACT (Continue on reverse if necessary and identify by block number)			
<p>A new inversion method, in which the frequency dependence of shear wave internal friction (<math>Q_u^{-1}</math>) is allowed to vary with depth, was developed and applied to selected Rayleigh wave attenuation data in the Basin and Range Province of the southwestern United States. Models were further constrained to satisfy observed values of <math>Q</math> and the frequency dependence of <math>L_g</math> waves in that region. Many models can explain those two data sets within their uncertainties, but at 1 Hz most have low values of <math>Q_u</math> (50-80) in the upper 8 km of the crust, rapidly increasing values to about 1000 at mid-crustal depths, and decreasing values at greater depths. Models which include a layer of higher <math>Q</math> values (80-150) in the upper few km of the crust, overlying a region of low <math>Q</math> values, cannot be predicted by the data of this study. Models for which the frequency dependence is low (0.0-0.1) in the upper crust best explain the available data. In the lower crust that frequency dependence may be substantial and leads to models in which <math>Q_u</math> may be an order of magnitude lower</p> <p style="text-align: right;">(continued)</p>			
20. DISTRIBUTION/AVAILABILITY OF ABSTRACT UNCLASSIFIED/UNLIMITED <input checked="" type="checkbox"/> SAME AS RPT. <input type="checkbox"/> DTIC USERS <input type="checkbox"/>		21. ABSTRACT SECURITY CLASSIFICATION	
22a. NAME OF RESPONSIBLE INDIVIDUAL Dr. Alan Ryall		22b. TELEPHONE NUMBER (Include Area Code) (703) 696-2245	22c. OFFICE SYMBOL

## 19. Abstract (continued)

( $\approx 100$ ) at a period of 100 s than it is at 1 s ( $\approx 1000$ ).

The low  $Q_u$  values, and their constancy with frequency, in the uppermost crust can be explained by fluid flow in a network of cracks in brittle rock. Increasing  $Q_u$  with depth to 10-15 km is caused by the increased closing of those cracks due to pressure and their enhanced healing with increasing temperature. Viscous flow at greater depths contributes further to the dissipation of cracks and to further increases in  $Q_u$ . Decreasing  $Q_u$  values at greater depths can be explained as the result of increasing temperature, increasing content of partial melt, enhanced dislocation motion, or some combination of these effects.

An Lg coda Q map has been derived for nearly all of Eurasia. Q values range from 1000 or more in stable region to 200 or less in regions having undergone recent tectonic activity. Q values in different shield regions differ, the maximum values being lower in the Siberian platform than those in the East European platform.

# TABLE OF CONTENTS

	page
Contributing Scientists	i
Publications	ii
Technical Summary	iii
Research Results	
Attenuation of Multiphase Surface Waves in the Basin and Range Province, Part III: Inversion for Crustal Anelasticity	1
Lg Attenuation across Northern Eurasia	37

DTIC QUALITY INSPECTED 5

<b>Accession For</b>	
NTIS GRA&I	<input checked="" type="checkbox"/>
DTIC TAB	<input type="checkbox"/>
Unannounced	<input type="checkbox"/>
Justification	
By	
Distribution/	
Availability Codes	
Dist	Avail and/or special
A-1	

**CONTRIBUTING SCIENTISTS**

B.J. Mitchell

Reinert Professor of Geophysics

J.K. Xie

Assistant Research Professor of Geophysics

Yu Pan

Graduate Student

Jianchuan Ni

Graduate Student

# PUBLICATIONS

The following manuscript was completed and submitted for publication. It uses observed values of fundamental-mode Rayleigh wave attenuation and 1 Hz Lg coda Q to place constraints on shear wave Q models for the crust in the Basin and Range province.

Mitchell, B.J., and J. Xie, Attenuation of multiphase surface waves in the Basin and Range province, Part III: Inversion for crustal anelasticity, Geophys. J. Int., submitted, 1992.

## TECHNICAL SUMMARY

A new inversion method, in which the frequency dependence of shear wave internal friction ( $Q_{\mu}^{-1}$ ) is allowed to vary with depth, was developed and applied to selected Rayleigh wave attenuation data in the Basin and Range Province of the southwestern United States. Models were further constrained to satisfy observed values of  $Q$  and the frequency dependence of  $Lg$  waves in that region. Many models can explain those two data sets within their uncertainties, but at 1 Hz most have low values of  $Q_{\mu}$  (50-80) in the upper 8 km of the crust, rapidly increasing values to about 1000 at mid-crustal depths, and decreasing values at greater depths. Models which include a layer of higher  $Q$  values (80-150) in the upper few km of the crust, overlying a region of low  $Q$  values, cannot be precluded by the data of this study. Models for which the frequency dependence is low (0.0-0.1) in the upper crust best explain the available data. In the lower crust that frequency dependence may be substantial and leads to models in which  $Q_{\mu}$  may be an order of magnitude lower ( $\approx 100$ ) at a period of 100 s than it is at 1 s ( $\approx 1000$ ).

The low  $Q_{\mu}$  values, and their constancy with frequency, in the uppermost crust can be explained by fluid flow in a network of cracks in brittle rock. Increasing  $Q_{\mu}$  with depth to 10-15 km is caused by the increased closing of those cracks due to pressure and their enhanced annealing with increasing temperature. Viscous flow at greater depths contributes further to the dissipation of cracks and to further increases in  $Q_{\mu}$ . Decreasing  $Q_{\mu}$  values at greater depths can be explained as the result of increasing temperature, increasing content of partial melt, enhanced dislocation motion, or some combination of these effects.

An Lg coda Q map has been derived for nearly all of Eurasia. Q values range from 1000 or more in stable regions to 200 or less in regions having undergone recent tectonic activity. Q values in different shield regions differ, the maximum values being lower in the Siberian platform than those in the East European platform.



**ATTENUATION OF MULTIPHASE SURFACE WAVES  
IN THE BASIN AND RANGE PROVINCE, Part III:  
INVERSION FOR CRUSTAL ANELASTICITY**

by

Brian J. Mitchell

and

Jia-kang Xie

Short Title: Q in the Basin and Range -- III

Department of Earth and Atmospheric Sciences  
Saint Louis University  
3507 Laclede Avenue  
St. Louis, MO 63103

## 1 INTRODUCTION

Records of surface waves at regional distances in continental regions typically consist of the short-period Lg phase, along with its coda, and longer period fundamental-mode waves. Modern broad-band digital seismic stations record these multiphase surface waves on the same data channel, even though their frequency contents are quite different. We presented, in earlier papers, results of our investigations of the dynamic properties of Lg and Lg coda (Xie and Mitchell, 1990) and of fundamental-mode surface waves (Mitchell *et al.*, 1992) and showed how they are affected by laterally complex structure in a region of the southwestern United States which includes the Basin and Range and adjacent tectonic provinces. These papers will hereafter be referred to as Part I and Part II, respectively.

When propagating through a laterally complex structure the dynamic properties of Lg and fundamental-mode surface waves are affected by various types of scattering produced by that complexity, as well as by intrinsic absorption of the medium. Ideally, we would like to isolate data which are affected solely, or at least predominantly, by intrinsic absorption, or anelasticity. The Q values which quantify that absorption are determined by such factors as temperature, and the amounts of fluid content, partial melt, or solid state dislocation motion in the crust or upper mantle. Knowledge of intrinsic Q values within the crust and upper mantle may therefore contribute

to our understanding of the tectonic evolution of regions where those values have been determined.

The acquisition of data sets which are suitable to invert for intrinsic anelasticity or  $Q$  requires great care. The sensitivity of  $Q$  measurements to particular kinds of lateral complexity can be quite different for different phases. It is important, therefore, when using these phases to study crustal  $Q$  structure, to understand possible biases which can affect them, and to either discard, or apply corrections to, data which are adversely affected by those biases.

Part I analyzed short-period Lg and Lg coda recorded by stations of the Lawrence Livermore National Laboratory (LLNL) network and resulted in highly consistent Lg  $Q$  ( $Q_{Lg}$ ) and Lg coda  $Q$  ( $Q_c$ ) values for a propagation path across the Basin and Range province. This was achieved using a carefully designed inverse scheme and a data selection procedure in which we reduced the effects of focusing/defocusing and non-flat site response on the Lg phase, and excluded those coda data which were significantly contaminated by scattering or by reflections from the coast line outside the LLNL network (Kennett *et al.*, 1990). Part II studied intermediate-period fundamental-mode surface wave propagation and showed that particle motion, and hence surface-wave amplitudes, were often adversely affected by major tectonic features such as coast lines or the Sierra Nevada, especially if

the surface waves impinged obliquely on those features. One path (ELK-MNV), however, which is sub-perpendicular to the Sierra Nevada, was found to provide unbiased data.

The present paper utilizes data from Part I and Part II, which were found to be unbiased, to invert for crustal anelasticity structure for the Basin and Range. Implicit in our inversion procedure is the assumption that  $Q$  measurements for both types of data are due to intrinsic shear-wave internal friction ( $Q_{\mu}^{-1}$ ) rather than to scattering. That this assumption is satisfied for long-period Rayleigh waves is apparent from the observation in Part II that retrograde-elliptical particle motion characterizes those waves along the selected path of study.  $Q_{Lg}$  and its frequency dependence along the selected path are also assumed to have been produced by intrinsic anelasticity effects. This conclusion is based upon the equivalence of  $Q_{Lg}$  and  $Q_c$  in Part I and on recent studies (e.g. Frankel and Wennerberg, 1987) which have found that coda  $Q$  is representative of intrinsic  $Q$ . Further support of that assumption is provided by the work of Jin and Aki (1988) who found that coda  $Q$  in a low- $Q$  region of China is likely to be measuring intrinsic  $Q$  and by Kennett (1990) who demonstrated theoretically that scattering contributes considerably less to apparent  $Q_{Lg}$  for a low  $Q$  environment than it does for a high- $Q$  environment.

This paper attempts to jointly utilize intermediate-period (6-33 s) fundamental-mode Rayleigh waves and  $Q_{Lg}$  at 1 Hz to obtain a model of shear wave internal friction for the crust and uppermost mantle of the Basin and Range province. We will utilize a new inversion method in which the frequency dependence of  $Q_{\mu}$  is allowed to vary with depth and we will assume that both Rayleigh wave attenuation and  $Q_{Lg}$  are dominated by intrinsic anelasticity rather than by scattering effects.

## 2 PREVIOUS CRUSTAL Q STUDIES IN THE BASIN AND RANGE

Previous studies of Q in the Basin and Range province using various wave types have all indicated that crustal Q values there are lower than in stable regions of North America. Sutton *et al.* (1967) found the first indication of low Q from the relative fall-offs of Pg and Lg energies for events in the Basin and Range and in the central United States. Mitchell (1975) obtained a model of crustal shear wave Q ( $Q_{\mu}$ ) for the western United States and found that differences in Rayleigh wave attenuation between the eastern and western United States could be explained by lower values of  $Q_{\mu}$  in the upper crust in the western United States. Cheng and Mitchell (1981), using a single-station multi-mode approach, found  $Q_{\mu}$  values in the upper crust of the Basin and Range to be about 85, as compared to about 275 in the central United States. Patton and Taylor (1984) inverted Rayleigh wave attenuation data obtained

over a broad portion of the Basin and Range and presented three  $Q_\mu$  models in which values in the upper crust ranged between about 110 and 170 and values in the lower crust which were substantially lower than those obtained by Mitchell (1975) and Cheng and Mitchell (1981). Lin (1989) inverted attenuation data obtained for a two-station path in the western Basin and Range and obtained  $Q_\mu$  values between about 40 and 60 in the upper crust and high values (1000 or more) at mid-crustal depths. A similar model obtained by Mitchell (1991) explains both fundamental Rayleigh mode attenuation and observed  $Lg$   $Q$  values.

A finding common to all of the crustal  $Q_\mu$  determinations in the Basin and Range province is that the upper crust has substantially lower  $Q_\mu$  values than those found in more stable regions. This low- $Q$  layer provides an explanation for the high relative attenuation of  $Lg$  reported for that region by Sutton *et al.* (1967) and is supported by subsequent determinations of  $Q$  for the  $Lg$  phase ( $Q_{Lg}$ ) and  $Lg$  coda ( $Q_c$ ) which are lower than for stable regions (e.g. Singh and Herrmann, 1983; Peseckis and Pomeroy, 1984; Chavez and Priestly, 1986; Nuttli, 1986).

### 3 FREQUENCY DEPENDENCES OF $Q_{Lg}$ AND $Q_\mu$

An expression for the internal friction of Rayleigh waves ( $Q_R^{-1}$ ) was given by Anderson *et al.* (1965). Using that expression,  $Q_R^{-1}$  can be obtained for any

Rayleigh mode if the appropriate velocities, partial derivatives of Rayleigh wave phase velocities with respect to shear- and compressional-wave velocities, and intrinsic  $Q_{\mu}^{-1}$  values are used. Mitchell (1980) extended that expression to incorporate  $Q_{\mu}$  values which vary with frequency. It is sometimes assumed that this frequency dependence of  $Q_{\mu}$  also pertains to  $Q_{Lg}$  (e.g. Campillo *et al.*, 1985; Herraiz and Espinosa 1987; Nuttli, 1986). Mitchell (1991) pointed out, however, that the frequency dependence of  $Q_R^{-1}$  can be caused by layering of the  $Q_{\mu}$  structure in the crust as well as by intrinsic frequency dependence of  $Q_{\mu}$ . He further showed that the frequency dependence of  $Lg$  observed in the Basin and Range province can be entirely explained by a layered model in which  $Q_{\mu}$  is independent of frequency and increases from low to high values at mid-crustal depths.

Frequency dependences of  $Q_{\mu}$  and  $Q_{Lg}$  are therefore fundamentally different parameters. In the sections that follow  $\zeta$  will refer to intrinsic frequency dependence of  $Q_{\mu}$  whereas  $\eta$  refers to frequency dependence of  $Q_{Lg}$  which is produced by the combined effects of intrinsic  $\zeta$  and changing values of  $Q_{\mu}$  with increasing depth in the crust.

#### 4 DATA

Data used to invert for crustal anelasticity in this study consist of fundamental-mode Rayleigh wave attenuation coefficient values from Part II

for the path between stations ELK and MNV (Figure 1). That path is sub-perpendicular to the major structural trends in the region and particle motion plots show that those values are not seriously affected by lateral refraction or multipathing of the Rayleigh waves. Those data were discussed in detail in Part II.

Further constraints on models obtained from the inversion of fundamental-mode data are provided by the Lg Q values and their frequency dependence obtained in Part I. After removing data for which Lg and its coda were adversely affected by portions of oceanic path, a very stable estimate was found for  $Q_{Lg}$  and its frequency dependence in the Basin and Range province. Using the relation  $Q_{Lg}(f) = Q_0 f^\eta$ , where  $Q_0$  is  $Q_{Lg}$  at 1 hz and  $\eta$  is a frequency dependence exponent, it was found in that  $Q_{Lg}(f) = (267 \pm 56)f^{(0.37 \pm 0.06)}$ . Since these values for  $Q_0$  and  $\eta$  are very similar to those found for coda Q along the same path, we inferred in Part I that they were produced by intrinsic anelasticity, rather than by scattering. Any model obtained from the inversion of fundamental-mode Rayleigh wave data should therefore predict a  $Q_0$  value of about 270 and a  $Q_{Lg}$  frequency dependence of about 0.4.

## 5 INVERSION PROCEDURE FOR $Q_\mu^{-1}$

The discussions in the previous section and in Parts I and II suggest that the



attenuation of both fundamental-mode Rayleigh waves and 1-Hz Lg waves in the crust of the Basin and Range province are dominated by intrinsic absorption. The same model of shear wave internal friction ( $Q_\mu^{-1}$ ) for that region should therefore explain both types of data.

Mitchell (1980) modified the equations of Anderson *et al.* (1965) to allow  $Q_\mu$  to vary with frequency,  $f$ , but restricted that frequency variation to be constant with depth. In the present study we allow that frequency dependence to vary with depth, so it can be written

$$Q_{\mu l} = Q_{0l} f^{z_l} \quad (1)$$

where the subscript  $l$  is a layer index and  $Q_{0l}$  is the  $Q_\mu$  value at 1 Hz for layer  $l$ . Toksöz *et al.* (1990) have previously allowed the frequency dependence of shear wave  $Q$  to vary with depth in a study in which they compared theoretical and observed seismograms at higher frequencies to infer an attenuation model for the crust in a high- $Q$  region.

We invert attenuation coefficient data ( $\gamma_R$ ) for  $Q_\mu^{-1}$  using

$$\gamma_R = \frac{\pi}{C_R^2 T} \sum_{i=1}^N \left[ \left( \beta_l \frac{\partial C_R}{\partial \beta_l} \right)_{\omega \rho \alpha} + \frac{1}{2} \left( \alpha_l \frac{\partial C_R}{\partial \alpha_l} \right)_{\omega \rho \beta} \right] Q_{\mu l}^{-1} \quad (2)$$

where the subscripts  $R$ ,  $\alpha$  and  $\beta$  identify Rayleigh, compressional, and shear waves, respectively,  $\omega$  is angular frequency, and  $C_R$  is Rayleigh wave phase velocity. When  $\omega$ ,  $\alpha$ , and  $\beta$  appear as subscripts, they indicate that those quantities are held constant when the partial derivatives are computed. The

factor  $\frac{1}{2}$  occurs in the right-hand term because we assume that compressional wave  $Q$  is twice as large as  $Q_\mu$  for all inversions of this study. Previous studies, such as Mitchell (1980), have indicated that inversion results are not strongly affected by the assumed value of compressional wave  $Q$ . Values for  $\alpha_1$  and  $\beta_1$  are taken from the Basin and Range model of Lin (1989) and values of  $\frac{\partial C}{\partial \alpha_1}$ ,  $\frac{\partial C}{\partial \beta_1}$ , and  $C_R$  are computed for that model.

The inversion process proceeds as follows:

1. Assume a depth distribution of  $\zeta_1$  and invert fundamental-mode Rayleigh-wave attenuation coefficients to obtain a  $Q_\mu^{-1}$  model for the Basin and Range.
2. Calculate the fundamental-mode Rayleigh wave attenuation coefficient values which are predicted by that model and compare with observed values. If they agree within the uncertainties of the data, go on to 3; if not, try a new distribution of  $\zeta_1$ .
3. Compute synthetic Lg seismograms at several distances from a seismic source using the velocity model of Lin (1989) and the  $Q_\mu^{-1}$  model resulting from the inversion of the fundamental-mode attenuation coefficient data. An example of several such synthetics at distances between 400 and 1200 km appears in Figure 2. In the inversions of the present study, we computed 20 seismograms evenly spaced at distances between 300

and 1250 km.

4. Apply the stacked spectral ratio (SSR) method of Xie and Nuttli (1988) to the set of synthetic Lg seismograms to obtain values of  $Q_0$  and  $\eta$  predicted by the derived  $Q_\mu^{-1}$  model, and compare those values with observed values of  $Q_0$  and  $\eta$  in the Basin and Range.

This process can be repeated from several different distributions of  $\zeta_1$  to obtain those models which best explain both the fundamental-mode Rayleigh wave attenuation data and the values of  $Q_0$  and  $\eta$  for Lg waves.

Our inversion procedure assumes a layered structure in which the number of layers exceeds the number of observed attenuation values. This makes the inversion of Rayleigh wave attenuation underdetermined and therefore non-unique. Non-uniqueness may be partly responsible for the differences between previously obtained models of  $Q_\mu$  (Patton and Taylor, 1984; Lin, 1989). The degree of non-uniqueness in the present study is higher than those in previous studies since, by allowing the frequency dependence of  $Q_\mu$  to vary with depth, we have introduced another set of parameters to the inversion process. Because of this non-uniqueness we have studied three classes of models to see how well they explain fundamental-mode Rayleigh wave attenuation and the  $Q$  and frequency dependence of 1-Hz Lg waves. The three classes of models are those in which (1)  $\zeta$  is uniform with depth, (2)  $\zeta$  increases from 0.0 in the upper crust to higher values at depth,

and (3)  $\zeta$  assumes positive values in the upper crust and decreases to 0.0 at depth.

An example of a model resulting from the inversion of Rayleigh wave attenuation data for the case of  $\zeta = 0.0$  at all depths appears in Figure 3. The effect which this model has on  $Q_{Lg}$  is discussed in the following section. The model is characterized by low  $Q_{\mu}$  values ( $\approx 50$ ) in the uppermost crust, high values ( $\approx 1000$ ) at mid-crustal depths, and decreasing  $Q_{\mu}$  values at greater depths. The resolving kernels to the right of the model indicate that resolution is best in the upper crust and degrades with increasing depth. At any depth, the value obtained is an average which is smeared out over the depth range of the resolving kernel. Those kernels indicate that only the gross features of the  $Q_{\mu}$  models can be resolved and any changes which occur over small depth ranges have no real meaning. The standard deviation bars associated with the model are small enough so that we can attribute significance to the major features. There is, of course, a preset parameter which allows us to trade off between resolution and standard deviation in the inversion process. We tried several settings for that parameter in each inversion and selected the model which best fit the Rayleigh wave attenuation data and, at the same time, did not lead to negative  $Q_{\mu}^{-1}$  values or wildly fluctuating changes between layers. Since all models of this study were obtained in this way the widths of the resolving kernels and standard deviations for all of

them are similar to those for the model in Figure 3.

## 6 INVERSION RESULTS

Models were first obtained in which the frequency dependence,  $\zeta$ , of  $Q_\mu$  was held at a uniform value for all depths. Three of those models, pertaining to a frequency of 1 Hz, appear in Figure 4 for  $\zeta = 0.0, 0.1$ , and  $0.2$ . All three models adequately explain fundamental-mode attenuation data (Figure 5), although the model for which  $\zeta = 0.2$  would predict an attenuation coefficient value which is slightly outside the standard deviation bar at 6 s. Values of  $Q_0$  and  $\eta$  predicted by the models also appear in the figure. The model in which  $\zeta = 0.1$  provides the best agreement with the observed value of  $Q_0$  (267) but predicts  $\eta$  values which are somewhat higher than the observed value of 0.37. The model in which  $\zeta = 0.0$  provides the best agreement with the observed  $\eta$  value but predicts a somewhat low  $Q_0$  value. Figure 5 compares values of Rayleigh wave attenuation coefficients predicted by models with  $\zeta$  values of 0.0, 0.5, and 1.0 with observed values. While all models predict attenuation coefficient values which lie within one standard deviation of mean observed values at periods greater than 8 s, only the curve for the model in which  $\zeta = 0.0$  lies within the standard deviations of observed values at shorter periods. These comparisons suggest that  $\zeta$  for this class of models must be about 0.2 or less. The  $Q_0$  and  $\eta$  values exhibited in Figure 4 also

imply that for models with a constant  $Q_\mu$  frequency dependence with depth,  $\zeta$  must be no greater than about 0.2.

The next group of models which we studied are those in which the frequency dependence of  $Q_\mu$  is 0.0 at shallow depths and assumes a higher value deeper in the crust. It was possible to find several models which predict  $Q_0$  and  $\eta$  values which are consistent with observed values. Figure 6 shows three of these and Figure 7 indicates how well they agree with observed Rayleigh wave attenuation coefficient values. A model in which  $\zeta = 0.0$  at depths between 0 and 15 km and  $\zeta = 0.5$  at greater depths produced  $Q_0$  and  $\eta$  values which are in excellent agreement with observed values. When  $\zeta$  at depth is increased to 1.0 a model in which that increase occurs at a depth of 18 km also provides good agreement between predicted and observed values of  $Q_0$  and  $\eta$  for Lg waves. When the  $\zeta$  increase is only to 0.2 the best fitting model is that for which the increase occurs at a depth of 8 km. That model predicts a  $Q_0$  value which is in excellent agreement with observed  $Q_0$  but it predicts an  $\eta$  value which is somewhat high. The models in which  $\zeta$  increases to 0.2 and to 0.5 both predict Rayleigh wave attenuation coefficient values which fall within, or are very close to, all observed standard deviations. The model in which  $\zeta$  increases to 1.0 at a depth of 18 km predicts a Rayleigh wave attenuation coefficient values which are somewhat low at periods of 6 and 8 s, but agree with observed values at all longer periods.

These results indicate that many models in which  $\zeta$  is small near the surface and increases at depth in the crust can explain both fundamental-mode Rayleigh wave attenuation coefficient data and  $Q_0$  and  $\eta$  values for Lg quite well. The degree of non-uniqueness in these inversions is, therefore, fairly large; a range of  $\zeta$  values can produce similar results. In addition the depth at which  $\zeta$  increases from zero to a positive value is not well resolved. For instance, if  $\zeta$  increases from 0.0 to 0.5, the depth at which that increase occurs can vary between about 10 and about 20 km and still satisfy fundamental-mode attenuation data, as well as  $Q_0$  and  $\eta$  values within their uncertainties.

Another group of models was studied in which  $\zeta$  assumed a positive value at shallow depths and changed to zero at greater depths in the crust. Figure 8 shows three models which explain most of the fundamental-mode attenuation coefficient data in Figure 9. There is little difference among the predicted attenuation coefficients predicted by the three models; they all predict values which are slightly high at periods of 8 and 10 s and slightly low at 6 s, but are in good agreement with all other data points. The model which yields the best value of  $Q_0$  was obtained for the case in which  $\zeta = 0.5$  between 0.0 and 6.0 km. That model also predicts a value of  $\eta$  which is within one standard deviation of the mean observation. When  $\zeta = 1.0$  at depths between 0.0 and 4.0 km, the resulting  $Q_\mu$  model also predicts  $Q_0$  and  $\eta$  values which are within observed standard deviations. Both of these

models are characterized by a high- $Q_\mu$  layer overlying a lower  $Q_\mu$  layer at greater depths. The third model, in which  $\xi = 0.2$  at depths between 0.0 and 8.0 km predicts a reasonable  $Q_0$  value but the  $\eta$  value is somewhat high.

These results indicate that models with a surface layer of moderately high  $Q_\mu$  values overlying a low- $Q_\mu$  layer do nearly as well as models without such a layer in explaining both fundamental-mode Rayleigh wave attenuation coefficient data and  $Q_0$  and  $\eta$  values for Lg. In an attempt to decide which of these two types of models is correct we computed synthetic seismograms for several models and compared them to observed seismograms which were obtained for paths entirely within the Basin and Range province (Figure 10). Those events for which seismograms were available are listed in Table 1 and their locations are shown in Figure 1. As shown in Figure 11, the model in which  $Q_\mu \approx 60$  in the uppermost crust and  $Q_\mu \approx 1000$  at mid-crustal depths produces Lg synthetics for which the envelopes are in good agreement with the observed wave forms in Figure 10. The only significant difference is that the codas in the observed wave forms continue to greater times than in the synthetics. Models in which  $Q_\mu^{-1} \approx 3.0 \times 10^{-3}$  ( $Q_\mu \approx 300$ ) in the upper 4 km of the crust (Figure 8) produce synthetic seismograms with a large phase which arrives about 40 s after the onset of Lg at a distance of 400 km and about 90 s after the onset of Lg at 750 km. No phase with such large amplitudes is present on any of the observed seismograms in Figure 10. The same



late phase is also present on the synthetic seismogram computed for a distance of 400 km for the model in which  $Q_{\mu}^{-1} \approx 7.5 \times 10^{-3}$  ( $Q_{\mu} \approx 130$ ), but has attenuated sufficiently so as to be nearly absent at a distance of 750 km. In the presence of noise or Lg coda produced by scattering it is possible that such a phase could be present but be undetectable. The computations indicate that  $Q_{\mu}$  in the upper crust of the Basin and Range cannot be as high as 300, but could be as high as 130 or slightly more.

The models plotted in Figures 4, 6, and 8 all give  $Q_{\mu}^{-1}$  values at 1 Hz. Since our inversion process yielded values of the frequency dependence of  $Q_{\mu}^{-1}$ , we can also determine models for other frequencies where intrinsic  $Q$  dominates seismic wave attenuation. Figure 12 shows  $Q_{\mu}$  models of the Basin and Range for periods of 1 s, 30 s, and 100 s for the case when  $\zeta = 0.1$  at all depths.  $Q_{\mu}$  becomes lower as period increases, being especially low ( $\approx 40$ ) in the upper crust at a period of 100 s. At mid-crustal depths, where  $Q_{\mu}$  is very high, there is little difference between the models for the three periods. At greater depths the difference increases but is much smaller than that at shallow depths.

For a model in which  $\zeta = 0.0$  between 0 and 15 km, and  $\zeta = 0.5$  at greater depths (Figure 13), the models are, of course, identical to a depth of 15 km, but show a large decrease of  $Q_{\mu}$  with increasing period at lower crustal and upper mantle depths. This frequency-dependent model exhibits the kind of

variation we would expect if viscous flow occurs in the lower crust and upper mantle;  $Q_\mu$  values would continue to decrease with increasing period and the anelasticity observed at seismic frequencies would be expected to merge into viscous flow at very large time scales.

## 7 DISCUSSION

### *Q Variation with Depth*

The  $Q_\mu$  models in Figures 4, 6, and 8 were obtained for a wide range of  $\zeta$  distributions with depth. Most of those distributions produced  $Q_\mu$  models which are similar in their major features --- low  $Q_\mu$  values in the upper crust, a high- $Q_\mu$  zone at mid-crustal depths, and lower  $Q_\mu$  values at greater depths. The only models which depart from that distribution are those in which  $\zeta$  is high in the uppermost crust. Such distributions produce a layer of high  $Q_\mu$  values in the upper few km of the crust. At depths of 8 km and greater, however, those models closely resemble models obtained from inversions using other  $\zeta$  distributions.

Models with near-surface layers in which  $Q_\mu$  values at 1 Hz are about 200 or more can be ruled out on the basis of our comparisons between synthetic and observed Lg seismograms. Models with more modest near-surface high- $Q_\mu$  layers, cannot, however, be ruled out on the basis of either our inversion results or seismogram comparisons. If we assume that  $Q_\mu$

distributions are similar throughout the western United States, however, a study by Hough and Anderson (1988) near Anza in southern California, seems to mitigate against such a layer. They found  $Q$  values in the upper 5 km of the crust (50-100) to be substantially lower than those between 5 and 15 km.

Low  $Q_\mu$  values in the upper crust have been attributed to the presence of fluids in a network of cracks (Mitchell, 1975, 1980) and is consistent with both laboratory results (Gordon and Davis, 1968) and theoretical predictions (O'Connell and Budiansky, 1977). Our results imply that fluids are present to 10 km or more in the crust. The high  $Q_\mu$  values at greater depths in our models imply that those fluids are absent at those depths. The prediction that those fluids are absent is consistent with the prediction of Bailey (1990) that free fluids have a short residence time in the ductile portion of the crust.

#### *Q Variation with Frequency*

The models which seem to best explain all available information are those in which  $Q_\mu$  values are low in the upper crust, increase rapidly to high values at mid-crustal depths, and decrease at greater depths. Inversions using a small uniform value of  $\zeta$  or inversions in which  $\zeta$  is small in the upper crust and increases to relatively large values at mid-crustal depth produce such models (Figures 4 and 6). The former  $\zeta$  distribution produces

models in which  $Q_\mu$  varies modestly with frequency at all depths (or not at all for  $\zeta = 0.0$ ), while the latter produces models which are independent of frequency in the upper crust and which exhibit a large variation of  $Q_\mu$  with frequency at greater depths. The lack of a frequency dependence for  $Q_\mu$  at upper crustal depths is consistent with laboratory results on samples which contain a network of fluid-filled cracks (Gordon and Davis, 1968) and is predicted theoretically for models in which fluid can flow in cracked solids (O'Connell and Budiansky, 1977).

At lower crustal depths  $Q_\mu$  at 100 s is much lower than  $Q_\mu$  at 1 s, being less by an order of magnitude at a depth of about 35 km. We would expect that type of behavior to occur if rock in the lower crust undergoes a transition from being solid, but anelastic, at seismic frequencies to exhibiting viscous flow at large time scales. This model predicts that seismic waves at 1 Hz will propagate efficiently through the lower crust, but that long-period waves will attenuate more rapidly.

It is interesting to compare this model with that of Toksöz *et al.* (1990) obtained using Rg waves recorded in the northeastern United States and both Rg and Lg waves in Scandinavia. Data in the two studies were, respectively at frequencies  $> 0.5$  Hz and  $> 1.0$  Hz; their model therefore pertains to higher frequencies than those of the present study. Their best-fitting models require (1) low  $Q_\mu$  values ( $< 100$ ), which increase with frequency as  $f^{0.5}$ , in

the upper crust. (2) moderate  $Q_\mu$  values (100-500), which increase with frequency as  $f^{1.0}$  at depths between 2 and 10 km, and (3) high  $Q_\mu$  values ( $\geq 500$ ), with indeterminate frequency dependence, in the lower crust. The pattern of increasing  $Q_\mu$  values with depth is similar to the findings of the present study, as well as earlier studies (e.g. Mitchell, 1975, 1980); the distribution of frequency dependence is, however, drastically different from that of the preferred model in the present study. The differences are undoubtedly due to the different frequency ranges of the data used in the two studies. Toksöz *et al.* (1990) explain the frequency dependence in the uppermost crust as being produced by fluid flow, but that dependence only occurs at frequencies above a critical frequency which may be as low as 1 Hz (Toksöz, *et al.*, 1987). Since our work utilized data at frequencies of 1 Hz and less, that frequency dependence is not expected to prevail in our study. The  $f^{1.0}$  frequency dependence of  $Q_\mu$  at depths between 2 and 10 km in the study of Toksöz *et al.* (1990) is explained as being due to scattering. Again, at the lower frequencies of the present study scattering effects are expected to be much less important. We find the greatest frequency dependence (in our preferred model) to occur in the lower crust, a region where the data of Toksöz *et al.* (1990) was unable to provide information.

*Relation of  $Q_\mu$  to Shear Strength in the Crust.*

Smith and Bruhn (1983) modeled the rheological behavior of the crust in the Basin and Range using shear stresses calculated at various depths for rock types expected to occur there, using thermal parameters from Lachenbruch and Sass (1977) and assuming a strain rate of  $10^{-15} \text{ s}^{-1}$ . They obtained a model for the eastern Basin and Range which included three brittle layers, the first at depths between 0 and 8 km, the second between 15 and 17 km, and the third between 25 and 27 km; ductile material lay beneath all of those layers. Their model for the central portion of the Basin and Range lacked the deeper two brittle layers. Since our  $Q_{\mu}$  model includes only one rapid increase with depth, it appears to correspond with the model of Smith and Bruhn (1983) for the central part of the Basin and Range.

The transition from brittle to ductile rock in the Basin and Range model of Smith and Bruhn (1983) is at a depth of 8 km. They indicate that, because of the uncertainty in the parameters used to derive their models, their models should be considered to be only rough guides to the rheological behavior of the crust. In another study, Jackson and McKenzie (1983) suggest that the brittle-ductile transition in extensional basins occurs somewhere in the depth range 10-15 km where temperatures are about 350°C. The difference between the Smith and Bruhn and Jackson and McKenzie models can be explained, at least partly, because the two studies make different assumptions as to the temperature at which the brittle-ductile transition occurs. Smith and Bruhn

take that temperature to be less than 300°C, or more than 50° cooler than that assumed by Jackson and McKenzie. Sibson (1984) showed that several factors, including temperature, crustal composition, fluid pressures in the frictional regime, water content in the ductile regime, and ductile strain rate, affect the depth to the transition. He pointed out, for instance, that the depth to the brittle-ductile transition was very dependent on the quartz content of rock in the brittle regime. Smith and Bruhn derived their model assuming that the upper crust corresponds to Westerly granite which includes about 30% quartz (Brace *et al.*, 1965). If the upper crust in the Basin and Range is comprised of rock with a lower quartz content, the brittle-ductile transition could occur at depths greater than 8 km.

Because of the uncertainty in the rheological properties in the Basin and Range we have compared our  $Q_\mu$  with two models, that of Smith and Bruhn (1983) in which the brittle-ductile transition occurs at a depth of 8 km and that of Jackson and McKenzine (1983) where it occurs in the depth range 10-15 km.

Figure 14 compares the  $Q_\mu$  model of our study with the model of shear strength,  $(\sigma_1 - \sigma_3)/2$ , of Smith and Bruhn (1983) and with a model for an extensional basin in which the brittle-ductile transition occurs at 12.5 km, the center of the range suggested by Jackson and McKenzie (1983). The three models are aligned with a histogram of earthquake focal depths for western

Nevada as compiled by Vetter and Ryall (1983). The depths are taken from Tables 2 and 3 of their paper.

A comparison of the  $Q_\mu$  model with the shear strength of Smith and Bruhn (1983) would suggest that only the range of decreasing  $Q_\mu^{-1}$  values ( $18$  to  $13 \times 10^{-3}$ ) between about 3 km and 8 km depth is caused by either crack closure and decrease of permeability caused by increasing pressure (Brace, 1980) or by the healing of cracks at elevated temperature (Smith and Evans, 1984). The latter process may occur at temperatures as low as 200°C in quartz. At depths greater than 8 km, the decrease in  $Q_\mu^{-1}$  ( $13$  to  $1 \times 10^{-3}$ ) would be due to crack closure through viscous flow as well as to decreased permeability and enhanced healing of cracks at higher pressures and temperatures. If the brittle-ductile transition lies at greater depths, more of the  $Q_\mu^{-1}$  decrease is caused purely by increased crack closure and healing. For the example in Figure 14, where the brittle-ductile transition is at a depth of 12.5 km, those factors cause  $Q_\mu^{-1}$  to decrease from  $18$  to  $7 \times 10^{-3}$  and the ductile flow contributes to the  $Q_\mu$  decrease from about  $7 \times 10^{-3}$  to about  $1 \times 10^{-3}$ .

The depth distribution of earthquakes in the western Basin and Range (Figure 14) appear to favor a rheological model in which the brittle-ductile transition is in the range 10-15 km as suggested by Jackson and McKenzie (1983) rather than at shallower depths. Only 27% of the earthquakes occur in the upper 8 km of the crust, whereas about 81% occur at depths of 14 km and



less. If we accept that model, partial crack closure by pressure and annealing are the factors which produce increases in  $Q_\mu$  to depths of 10-15 km and viscous flow is an additional contributing factor at greater depths.

At depths greater than about 25 km,  $Q_\mu^{-1}$  values increase with depth. The effect of temperature on  $Q_\mu$  at those depths can be computed using a formulation due to Anderson and Archambeau (1964). It is an easy matter to describe the  $Q_\mu$  decrease using that formulation, by selecting various values for activation energies and activation values for  $Q_\mu$ . Correct values for those parameters are not known, however, so we will not present the results of those calculations, but simply indicate that various combinations of those parameters can achieve the desired result. Other factors which may contribute to the increase in  $Q_\mu^{-1}$  at these depths are partial melt (Shankland *et al.*, 1981) and enhanced dislocation motion (Minster and Anderson, 1980).

## 8 CONCLUSIONS

Various assumed distributions of  $Q_\mu$  frequency dependence produce somewhat different  $Q_\mu$  models for the crust of the Basin and Range province. Many models explain the observed attenuation of fundamental-mode Rayleigh waves as well as  $Q$  and its frequency dependence for 1-Hz Lg waves. Most models, however, have the common features of low  $Q_\mu$  values (50-80) at depths between 0 and 8 km, rapidly increasing values at mid-crustal depths

reaching a maximum at a depth of about 20 km, and decreasing values at greater depths. Models in which the upper crust has a layer of higher  $Q_\mu$  values (80-150) overlying a low- $Q_\mu$  region can also explain available data, but are inconsistent with results of  $Q$  studies in nearby regions. The frequency dependence of  $Q_\mu$  in the upper crust must be low (0.0 - 0.1), but it may be substantially higher (as much as 1.0) in the lower crust. A model in which that frequency dependence is 0.5 leads to a model in which  $Q_\mu$  can be an order of magnitude lower ( $\approx 100$ ) at 100 s than it is at 1 s ( $\approx 1000$ ).

The low  $Q_\mu$  values in the uppermost crust are most easily explained as being due to a network of fluid-filled cracks which permeates brittle rock in that depth range. Increasing closure of those cracks by pressure and annealing effects causes  $Q_\mu$  to increase with increasing depth. They are the dominant effects until the brittle-ductile transition is reached where crack closure due to viscous flow becomes important. The depth of that transition is not well determined, but the distribution of focal depths in the western Basin and Range favors its occurrence in the range 10-15 km. Decreasing  $Q_\mu$  at depths greater than 25 km may be caused by increasing temperature, increasing presence of partial melt, enhanced dislocation motion or some combination of these effects.

#### ACKNOWLEDGMENTS

We thank Fred Chester for several valuable comments during the course of this work. This research was supported by the Defense Advanced Research Projects Agency of the Department of Defense and was monitored by the Air Force Geophysics Laboratory under contract F29601-91-K-DB19.

## REFERENCES

- Anderson, D.L. & Archambeau, C.B., 1964. The anelasticity of the Earth, *J. Geophys. Res.*, 69, 2071-2084.
- Anderson, D.L., Ben-Menahem, A. & Archambeau, C.B., 1965. Attenuation of seismic energy in the upper mantle, *J. Geophys. Res.*, 70, 1441-1448.
- Brace, W.F., 1980. Permeability of crystalline and argillaceous rocks, *Int. Rock Mech. Mineral Sci.*, 17, 241-251.
- Brace, W.F., Orange, A.S. & Madden, T.R., 1965. The effect of Pressure on the electrical resistivity of water-saturated crystalline rocks, *J. Geophys. Res.*, 70, 5669-5678.
- Campillo, M., Plantet, J., & Bouchon, M., 1985. Frequency-dependent attenuation in the crust beneath central France from Lg waves: Data analysis and numerical modeling, *Bull. Seism. Soc. Am.*, 75, 1395-1411.
- Chavez, D.E. & Priestley, K.F., 1986. Measurement of frequency dependent

- Lg attenuation in the Great Basin, *Geophys. Res. Lett.* 13, 551-554.
- Cheng, C.C. & Mitchell, B.J., 1981. Crustal Q structure in the United States from multi-mode surface waves, *Bull. Seism. Soc. Am.*, 71, 161-181.
- Gordon, R.B. & Davis, L.A., 1968. Velocity and attenuation in imperfectly elastic rock, *J. Geophys. Res.*, 73, 3917-3935.
- Herraiz, M. & Espinosa, A.F., 1987. Coda waves: A review, *PAGEOPH*, 125, 499-578.
- Hough, S.E. & Anderson, J.G., 1988. High-frequency spectra observed at Anza, California: Implications for Q structure, *Bull. Seism. Soc. Am.*, 78, 692-707.
- Jackson, J. & McKenzie, D. 1983. The geometrical evolution of normal fault systems, *J. Struct. Geol.*, 5, 471-482.
- Jin, A. & Aki, K., 1988. Spatial and temporal correlation between coda Q and seismicity in China, *Bull. Seism. Soc. Am.*, 78, 741-769.
- Kennett, B.L.N., 1990. Guided wave attenuation in laterally varying media, *Geophys. J. Int.*, 100, 415-422.
- Kennett, B.L.N., Bostock M.G. & Xie, J.K., 1990. Guided wave tracking in

- 3-D: A tool for interpreting complex regional seismograms, *Bull. Seism. Soc. Am.*, 80, 633-642.
- Lachenbruch, A.H. & Sass J.H., 1977. Heat flow in the United States and the thermal regime of the crust, in *The Earth's Crust, Geophys. Monogr. Ser.*, 20, edited by J.G. Heacock, AGU, Washington, DC, 626-675.
- Lin, W.J., 1989. Rayleigh Wave Attenuation in the Basin and Range province, M.S. Thesis, Saint Louis University, 55 pp.
- Minster, J.B. & Anderson, D.L., 1980. Dislocations and nonelastic processes in the mantle, *J. Geophys. Res.*, 85, 6347-6352.
- Mitchell, B.J., 1975. Regional Rayleigh wave attenuation in North America, *J. Geophys. Res.*, 80, 4904-4916.
- Mitchell, B.J., 1980. Frequency dependence of shear wave internal friction in the continental crust of eastern North America, *J. Geophys. Res.*, 85, 5212-5218.
- Mitchell, B.J., Xie, J.K. & Lin, W.J., 1992. Attenuation of multiphase surface waves in the Basin and Range province, Part II: The fundamental mode, *Geophys. J. Int.*, submitted.
- Nuttli, O.W., 1986. Yield estimates of Nevada Test Site explosions obtained

from seismic Lg waves, *J. Geophys. Res.*, 91, 2137-2152.

O'Connell, R.J. & Budiansky, B., 1977. Viscoelastic properties of fluid-saturated cracked solids, *J. Geophys. Res.* 82, 5719-5735.

Patton, H.J. & Taylor, S.R., 1984. Q structure of the Basin and Range from surface waves, *J. Geophys. Res.*, 89, 6929-6940.

Peseckis, L.L. & Pomeroy, P.W., 1984. Determination of Q using Lg waves and its implications for nuclear yield estimation, *EOS, Trans. Am. Geophys. Union*, 65, 995.

Shankland, T.J., O'Connell, R.J. & Waff, H.S., 1981. Geophysical constraints on partial melt in the upper mantle, *Rev. Geophys. Space Phys.*, 19, 394-406.

Sibson, R.H., 1984. Roughness at the base of the seismogenic zone: Contributing factors, *J. Geophys. Res.*, 89, 5791-5799.

Singh, S.K. & Herrmann, R.B., 1983. Regionalization of crustal coda Q in the continental United States, *J. Geophys. Res.*, 88, 527-538.

Smith, D.L. & Evans, B., 1984. Diffusional crack healing in quartz, *J. Geophys. Res.*, 89, 4125-4135.

Smith, R.B. & Bruhn, R.L., 1984. Intraplate extensional tectonics of the

- eastern Basin-Range: Inferences on structural style from seismic reflection data, regional tectonics, and thermal-mechanical models of brittle-ductile deformation, *J. Geophys. Res.*, 89, 5733-5762.
- Sutton, G.H., Mitrovic, W. & Pomeroy, P.W., 1967. Short-period seismic energy radiation patterns from underground nuclear explosions and small-magnitude earthquakes, *Bull. Seism. Soc. Am.*, 57, 249-267.
- Toksöz, M.N., Wu, R.S. & Schmitt D.P., 1987. Physical mechanisms contributing to seismic attenuation in the crust, Proc. NATO ASI "Strong Ground Motion Seismology," Ankara, Turkey, 225-247.
- Toksöz, M.N., Mandal, B. & Dainty, A.M., 1990. Frequency dependent attenuation in the crust, *Geophys. Res. Lett.*, 17, 973-976.
- Vetter, V.R. & Ryall, A.S., 1983. Systematic change of focal mechanism with depth in the western Great Basin, *J. Geophys. Res.*, 88, 8237-8250.
- Wang, C.Y., 1981. Wave Theory for Seismogram Synthesis, Ph.D. Dissertation, Saint Louis University, 235 pp.
- Xie, J.K. & Nuttli, O.W., 1988. Interpretation of high-frequency coda at large distances: stochastic modelling and method of inversion, *Geophys. J.*, 95, 579-595.

Xie, J.K. & Mitchell, B.J., 1990. Attenuation of multiphase surface waves in the Basin and Range province, Part I: Lg and Lg coda, *Geophys. J. Int.*, 102, 121-137.



## FIGURE CAPTIONS

Figure 1. Map of a portion of the Basin and Range province (denoted by the heavy line) showing the locations of stations MNV and ELK used to obtain fundamental-mode Rayleigh-wave attenuation coefficients used to invert for internal friction models. The X symbols indicate epicenters of the earthquakes listed in Table 1 and for which seismograms are plotted in Figure 10.

Figure 2. Synthetic seismograms computed by modal summation (wang, 1981) for distances between 400 and 1200 km. The seismograms were computed along an azimuth of  $45^\circ$  from a vertical strike-slip fault at a depth of 5 km and oriented in a north-south direction. The time scale is reduced at each distance R using a reduction velocity of 5.0 km/s.

Figure 3. (Left)  $Q_\mu^{-1}$  model at 1 Hz obtained from the inversion of fundamental-mode attenuation coefficients for the path between stations ELK and MNV assuming that the  $Q_\mu$  frequency-dependence exponent ( $\zeta$ ) is 0.0 at all depths. Horizontal lines denote one standard deviation. (Right) Normalized resolving kernels determined for depths of 3.0, 9.0, 19.5, and 28.5 km.

Figure 3. Synthetic seismograms computed by modal summation (Wang,

1981) for distances between 400 and 1200 km. The seismograms were computed along an azimuth of  $45^\circ$  from a vertical strike-slip fault at a depth of 5 km and oriented in a north-south direction. The time scale is reduced at each distance  $R$  using a reduction velocity of 5.0 km/s.

Figure 4. Models of shear-wave internal friction at 1 Hz (left) resulting from the inversion of fundamental-mode Rayleigh-wave attenuation coefficients for three models for which the frequency dependence of internal friction (right) is uniform with depth and takes on values of 0.0, 0.1, or 0.2. Values of  $Q_{Lg}$  and its frequency dependence at 1 Hz are listed for each model.

Figure 5. Comparison of Rayleigh-wave attenuation coefficient values, predicted by models in which  $\zeta$  is uniform with depth and takes on values of 0.0, 0.5, and 1.0, with observed values.

Figure 6. Models of shear-wave internal friction at 1 Hz (left) resulting from the inversion of fundamental-mode Rayleigh-wave attenuation coefficients for three models for which the frequency dependence of internal friction (right) increases from 0.0 to a positive value (0.2, 0.5, or 1.0) at mid-crustal depths. Values of  $Q_{Lg}$  and its frequency dependence at 1 Hz are listed for each model.

Figure 7. Comparison of Rayleigh-wave attenuation coefficient values predicted by the model in Figure 6 with observed values. The solid and dashed lines correspond to similar lines representing the models in Figure 6.

Figure 8. Models of shear-wave internal friction at 1 Hz (left) resulting from the inversion of fundamental-mode Rayleigh-wave attenuation coefficients for three models for which the frequency dependence of internal friction (right) decreases from a positive value (0.2, 0.5, or 1.0) to 0.0. Values of  $Q_{Lg}$  and its frequency dependence at 1 Hz are listed for each model.

Figure 9. Comparison of Rayleigh-wave attenuation coefficient values predicted by the model in Figure 8 with observed values. Predicted values for the three models are nearly indistinguishable.

Figure 10. Seismograms from the broad-band stations ELK and MNV for the events of Table 1 and Figure 1 after being high-pass filtered above 0.3 Hz.

Figure 11. Synthetic Lg seismograms corresponding to paths between the events shown in Figure 1 and the stations ELK and MNV. (Top) Seismograms predicted by the model in Figure 6 in which  $Q_{\mu}^{-1}$  in the uppermost crust is about  $17.5 \times 10^{-3}$  ( $Q_{\mu} \approx 60$ ) with higher values at greater depths. (Middle) Seismograms predicted by the model in Figure 8 in which  $Q_{\mu}^{-1}$  in

the uppermost crust is about  $3 \times 10^{-3}$  ( $Q_\mu \approx 300$ ) with lower values of  $Q_\mu$  at greater depths. (Bottom) Seismograms predicted by the model in Figure 9 in which  $Q_\mu^{-1}$  in the uppermost crust is about  $7.5 \times 10^{-3}$  ( $Q_\mu \approx 130$ ) with lower values of  $Q_\mu$  at greater depths.

Figure 12. Frequency-dependent  $Q_\mu^{-1}$  model of the crust in the Basin and Range when the frequency-dependence exponent ( $\zeta$ ) is constant with depth and has a value of 0.1.

Figure 13. Frequency-dependent  $Q_\mu^{-1}$  model of the crust in the Basin and Range when the frequency-dependence exponent ( $\zeta$ ) has the value of 0.0 at depths between 0 and 15 km and has the value of 0.5 at greater depths.

Figure 14. a. Histogram of earthquake activity at 2 km intervals in the western Basin and Range (from Vetter and Ryall, 1983). b.  $Q_\mu^{-1}$  model of the Basin and Range. c. Model of shear strength obtained by Smith and Bruhn (1983) for the central part of the Basin and Range. d. Model of shear strength for extensional basins by Jackson and McKenzie (1983), taking the brittle-ductile transition to be at 12.5 km. Stippling represents the brittle portion of the crust.

### Lg ATTENUATION ACROSS NORTHERN EURASIA

We have mapped Lg coda Q and its frequency dependence throughout northern Eurasia, including the Barents shelf. Those results, when combined with a similar map for southern Eurasia (Xie and Mitchell, 1991) provide Lg coda Q and frequency dependence values which cover most of the continent, from the Arctic regions of Europe to southern Asia as far south as 20° north latitude. Our Q map for Eurasia, derived from data processed up to now, appears in Figure 1.

Our map of Eurasia shows Q values generally decrease from north to south from a high of about 1000 to about 200. Low values (200-300) occur in a broad zone which stretches across western China, northern India, and adjacent portions of central Asia. Localized regions of low Q lie within, and near, the Caspian Sea and western Turkey. The highest values occur in stable regions and the lowest values occur in regions of recent tectonic activity, results which are consistent with our earlier studies in other regions.

It is interesting that Q values for the region of the Siberian platform (higher than average values in the northeastern portion of the map) are lower than those for the East European platform (high values in the northwestern portion of the map). These low values may reflect intraplate tectonism in that platform which occurred at a time which postdates the accretion of the subplates which formed Eurasia.

Work is continuing on this map. Data from a recent moderately large earthquake in the Netherlands recorded at several European stations, and data from Novaya Zemlya explosions recorded at Arcess and Noress are

currently being processed. When that is completed, estimates of resolution and error in the measurements will be obtained.